Life Sciences 239 (2019) 117073

Contents lists available at ScienceDirect

Life Sciences

journal homepage: www.elsevier.com/locate/lifescie

Genistein potentiates Centchroman induced antineoplasticity in breast cancer *via* PI3K/Akt deactivation and ROS dependent induction of apoptosis

Shweta Kaushik[a,b,1], Hari Shyam[a], Satish Agarwal[c], Ramesh Sharma[a], Tapas C. Nag[d], Anil K. Dwivedi[c], Anil K. Balapure[a,b,*]

[a] Division of Biochemistry, CSIR-Central Drug Research Institute, Lucknow 226031, India
[b] Academy of Scientific and Innovative Research, Taramani, Chennai 600113, India
[c] Division of Pharmaceutics, & Pharmacokinetics, CSIR-Central Drug Research Institute, Lucknow 226031, India
[d] Department of Anatomy, All India Institute of Medical Sciences, New Delhi 110029, India

ARTICLE INFO

Keywords:
Breast Cancer
Centchroman
Ormeloxifene
Genistein
PI3K/Akt
Apoptosis

ABSTRACT

Aims: Recently, strategies of cancer treatment using combination of agents with distinct molecular mechanism (s) of action are considered more promising due to its high efficacy and reduced systemic toxicity. The study is aimed to improve the efficacy of selective estrogen receptor modulator, Centchroman (CC) by combination with the phytoestrogen Genistein (GN).

Methods: Cytotoxicity was evaluated by Sulforhodamine B assay. Cell cycle analysis was done through flow cytometry. Further, Apoptosis was analyzed using Annexin V/PI staining, tunel assay and electron microscopic examination and verified using western blot analysis. In order to validate the *in vitro* results, *in vivo* analysis was performed using 4T1-syngeneic mouse model.

Key findings: In this study, we report that the dietary isoflavone genistein (GN) synergistically improved antineoplasticity of CC in breast cancer by arresting cells at G2/M phase culminating in ROS dependent apoptosis. The combination of CC plus GN caused dysregulation of Bax and Bcl-2 ratio inducing mitochondrial dysfunction, activation of Caspase-3/7, -9 and PARP cleavage. Further, combination significantly suppresses phosphorylation of PI3K/Akt/NF-κB, enhancing apoptosis. Additionally, combination markedly reduced tumor growth compared to CC and GN alone in mouse 4T1 breast tumor model.

Significance: Together, these studies suggest that GN represents a potential adjunct molecule whose role in CC induced apoptosis deserves attention.

1. Introduction

Despite remarkable progress in cancer diagnostics, treatment of breast cancer (BC) remains a higher challenge and enigma [1]. This is perhaps due to the chemo-resistant nature of BC towards various chemotherapeutic agents or radiotherapy [2]. Besides, development of systemic cytotoxicity poses severe limitations on the anti-cancer efficacy of chemotherapy. Centchroman (CC), a non-steroidal oral contraceptive is a type of selective estrogen receptor modulator, having estrogen antagonist action in breast, ovary and uterus & agonistic in bone [3]. We and others have demonstrated its anticancer action against various malignancies including breast, endometrial, pancreatic and head & neck cancer [4–8].

Phytoestrogen genistein (GN), a prominent isoflavone of soy has received great attention due to its explicit and almost exclusive activity on cancer cells rather than non-transformed and normal cells. Several *in vitro* and *in vivo* studies have shown that GN inhibits the proliferation of many cancer cells through cell cycle arrest (G2/M) by decreasing cyclin B1, cdc 2 expression and induction of apoptosis by activation of caspase-9 &-3 [9]. Studies have shown that defects in the genes and multiple signaling pathways are the major cause of cancer therefore; a combination of agents which targets several signaling pathways without causing any systemic toxicity would be a promising strategy for cancer prevention. Various studies have demonstrated that GN prevents the growth and proliferation of cancer cells by synergistically ameliorating the effect of anticancer drugs [10–12].

* Corresponding author at: Division of Biochemistry, CSIR-Central Drug Research Institute, Sector -10, Jankipuram Extension, Lucknow, Uttar Pradesh 226031, India.
E-mail address: anilbalapure58@gmail.com (A.K. Balapure).

[1] Recipient of a research fellowship from University Grants Commission (UGC), New Delhi and this work constitutes a part of her PhD thesis.

https://doi.org/10.1016/j.lfs.2019.117073
Received 30 July 2019; Received in revised form 28 October 2019; Accepted 14 November 2019
Available online 19 November 2019
0024-3205/

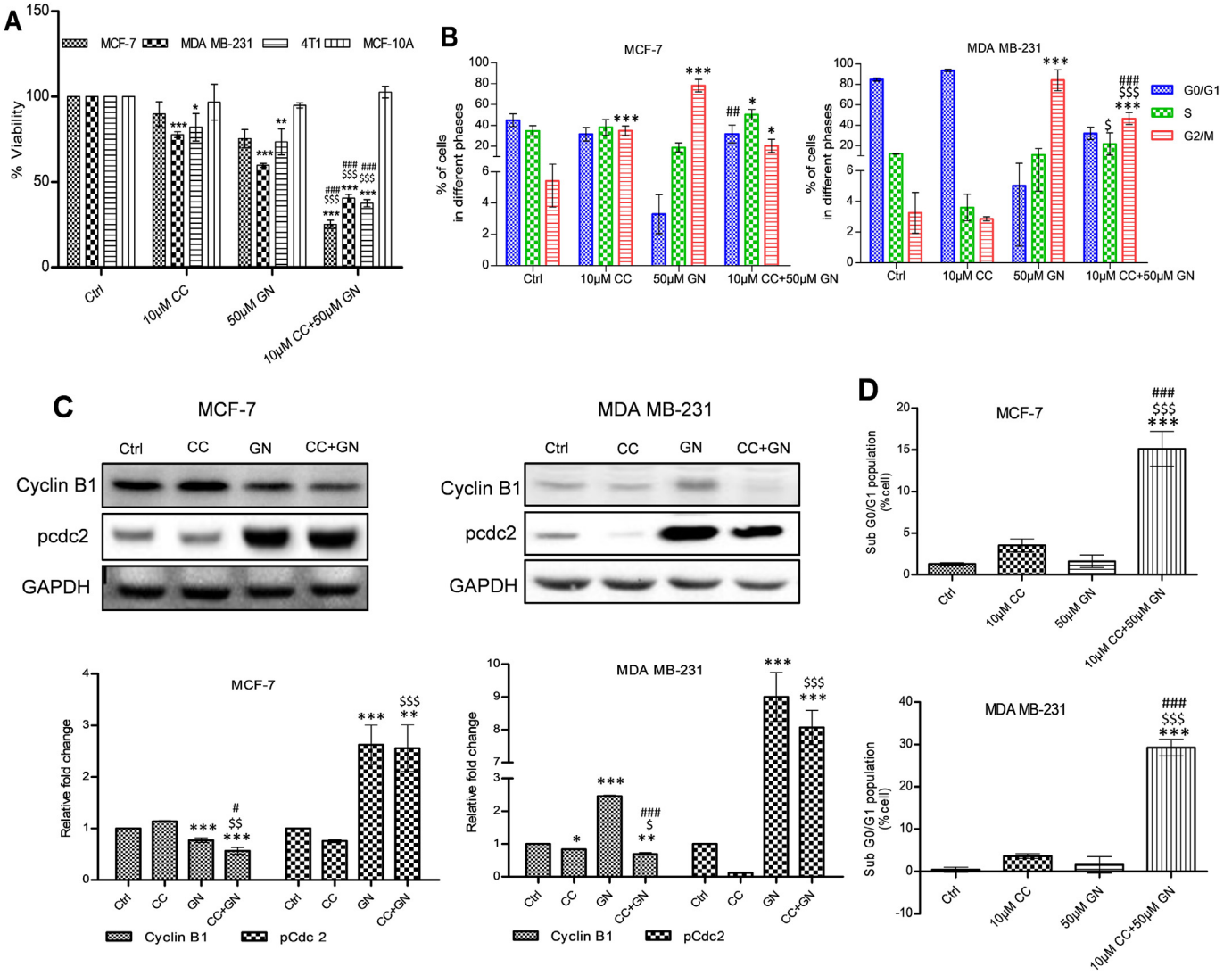

Fig. 1. CC and GN synergistically inhibits proliferation of HBCCs. (A) Cytotoxicity analysis of 10 μM CC and 50 μM GN separately and together in MCF-7/MDA MB-231, 4T1 and MCF-10A cells. (B) Cell cycle analysis was performed using flow cytometry in MCF-7/MDA MB-231 cells treated with 10 μM CC & 50 μM GN separately and together. (C) Western blot analysis of the indicated proteins, GAPDH was used as loading control. (D) Graphical representations indicating normalized relative band intensity. $^{*}p < 0.05$; $^{**}p < 0.01$; $^{***}p < 0.001$, calculated compared to control. $\$p < 0.05$; $\$\$p < 0.01$; $\$\$\$p < 0.001$ with respect to CC alone and $\#p < 0.05$; $\#\#p < 0.01$; $\#\#\#p < 0.001$ with respect to GN alone.

The rationale behind the present study is to evaluate the efficacy of the dietary GN in improving CC action in Human Breast Cancer Cells (HBCCs). Our previous study suggests that GN potentiates CC action in HBCCs where the exact molecular pathway of synergism remains unelucidated [13]. Here, our results demonstrate that the combination of CC plus GN arrests cells at G2/M phase and induces apoptosis by down-regulating expression of Bcl-2, Akt, NF-κB and up-regulating Bax, Caspase-3/7& -9. The results obtained *in vitro* are remarkably supported by the tumor regression in combination group in mouse 4T1 breast tumor model. Together, our data illustrates that CC plus GN possesses considerably high anticancer potential which combination may offer greater therapeutic response to the adenocarcinoma of the breast.

2. Materials and methods

2.1. Reagents

Dulbecco's Modified Eagle's Medium (DMEM), Genistein, Trypsin, Sulforhodamine B (SRB), Bovine Serum Albumin (BSA), Anti-pCdc2 (Cdk1) (pTyr15), Anti-Cyclin B1 were procured from Sigma Aldrich (St. Louis, MO 63103 USA). Anti-Bcl-2, Anti-Bax, Anti-Bcl-xL, Anti-AIF, Anti-Cleaved PARP, Anti-CuZnSOD, Anti-MnSOD, Anti-Catalase, Anti-Caspase-3, -8 & -9 (active) were purchased from BioVision Research Product (Mountain View, CA 94043 USA). Anti-pNF-κB, Anti-PI3K, Anti-pAkt, Anti-Akt and Anti-pmTOR, mTOR and Anti-GAPDH were procured from Santa Cruz Biotechnology (Texas 75220, USA.). CC was obtained from CSIR-Central Drug Research Institute, Lucknow (Uttar Pradesh), India.

2.2. Cell culture

MCF-7/MDA MB-231 cells were procured from National Centre for Cell Sciences, Pune. MCF-10A and 4T1 cells were obtained from American Type Culture Collection (ATCC, Manassas, VA). All the cells were cultured as described previously [13,14].

2.3. Evaluation of cell viability

Sulforhodamine B (SRB) assay was performed for the analysis of cell viability. Briefly, 1×10^4 cells were cultured in DMEM/F-12 medium

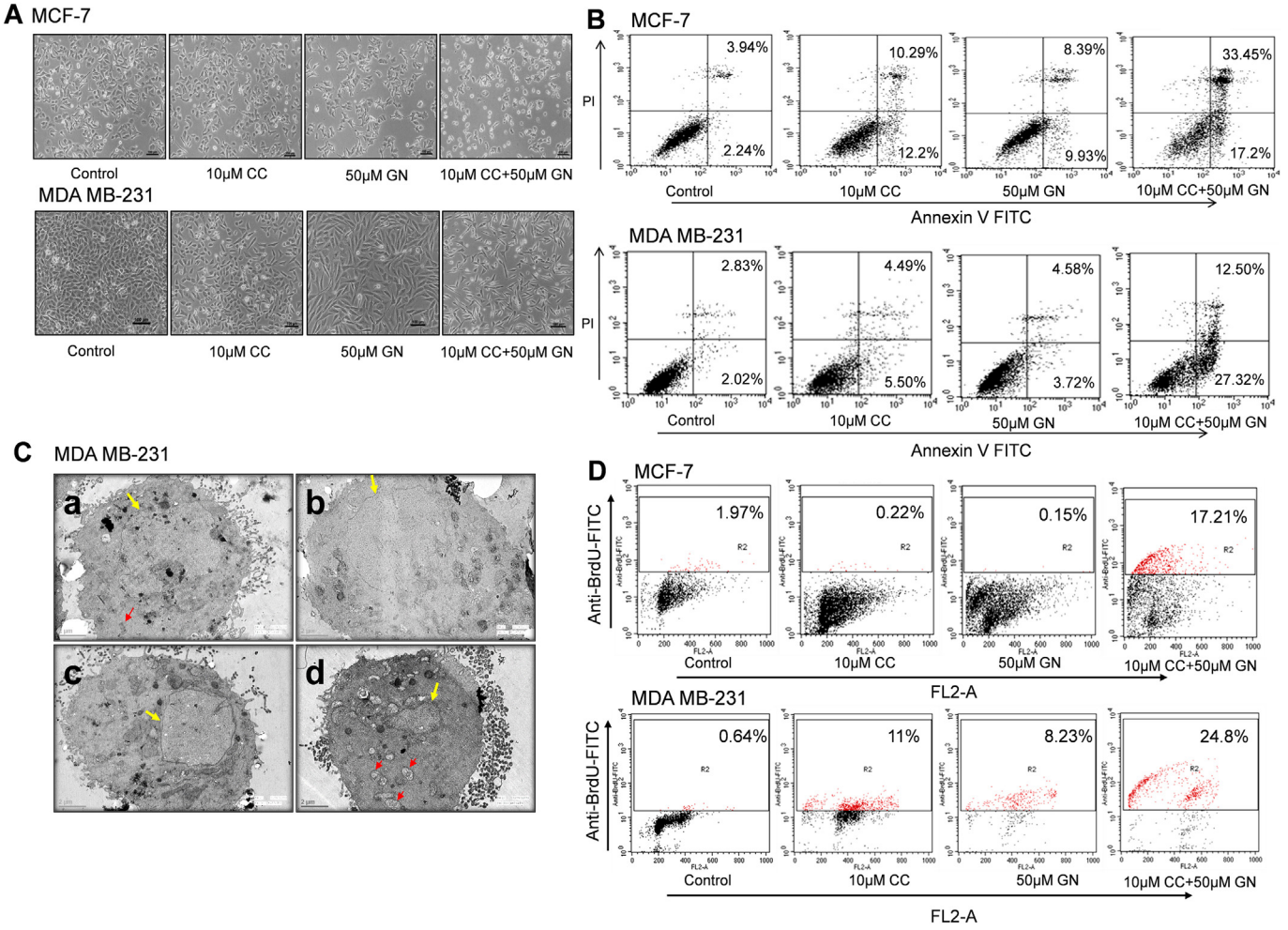

Fig. 2. Combination induces apoptosis in HBCCs. (A) Morphological analysis of MCF-7/MDA MB-231 cells treated with 10 μM CC & 50 μM GN separately and together. (Scale bar = 100 μm) (B) Post-drug treatment, cells were stained with Annexin V/PI and analyzed through flow cytometry (C) Transmission electron microscopic analysis of MDA MB-231 cells (a) control (b) 10 μM CC (c) 50 μM GN (d) 10 μM CC plus 50 μM GN. Yellow and red arrows indicating nucleus and mitochondria respectively (Scale bar = 2 μm). (E) Tunel assay was performed after incubating HBCCs with the respective doses and analyzed using flow cytometry. Data shown are representative of three similar experiments. (For interpretation of the references to colour in this figure legend, the reader is referred to the web version of this article.)

and exposed with 10 μM CC & 50 μM GN separately and together for 48 h. Thereafter, SRB assay was performed as before [13] and absorbance was measured in SpectraMaxM2^{e}Elisa Microplate Reader (Molecular Devices Inc.) at 510 nm.

2.4. Analysis of cell cycle kinetics

To assess cell cycle, MCF-7/MDA MB-231 cells were placed in 6-well plate and exposed to 10 μM CC and 50 μM GN separately and together. After 48 h, cells were permeabilized and re-suspended in PBS containing PI (40 μg/ml) and RNase (100 μg/ml). Flow cytometry analysis was performed on FACS Calibur employing CellQuest Software (Becton Dickinson, San Jose, CA, USA) [15].

2.5. Annexin V/PI binding assay

Annexin-V apoptosis detection kit (Sigma Chemical Co. St. Louis, MO, USA) was used to analyze the exposure of phosphatidylserine at the cell surface. Briefly, 0.2 × 10^6 cells were plated in 6-well plate, exposed with 10 μM CC & 50 μM GN separately and together for 48 h. Apoptotic cells were analyzed after double staining the cells with FITC conjugated Annexin V and propidium iodide (PI) through flow cytometry.

2.6. TUNEL assay

To examine DNA fragmentation, TUNEL assay was performed using ApoDIRECT *In Situ* DNA Fragmentation/Assay Kit (Biovision, Milpitas, CA 95035, USA) according to manufacturer's protocol. MCF-7/MDA MB-231 cells (0.2 × 10^6) were cultured in 6-well plates, incubated with 10 μM CC & 50 μM GN separately and together for 48 h. Thereafter, staining was done according to the protocol and cells were analyzed by flow cytometry [7].

2.7. Detection of intracellular reactive oxygen species (ROS) generation

Time-dependent ROS was quantified post-drug challenge in HBCCs after 6, 12 & 24 h. Briefly, 0.2 × 10^6 cells were plated in 6-well plate exposed to respective doses for 6, 12 & 24 h. Subsequently, cells were washed with PBS, incubated with 10 μM 2′,7′ Dichlorofluorescein diacetate (DCFDA) at 37 °C for 30 min in the dark and analyzed through flow cytometry (FACS Calibur employing CellQuest Software) [15].

2.8. Analysis of mitochondrial membrane potential (MMP)

Alteration in MMP was evaluated using MitoTracker® Deep Red FM (Life Technologies, Eugene, OR, USA) per the manufacturer's

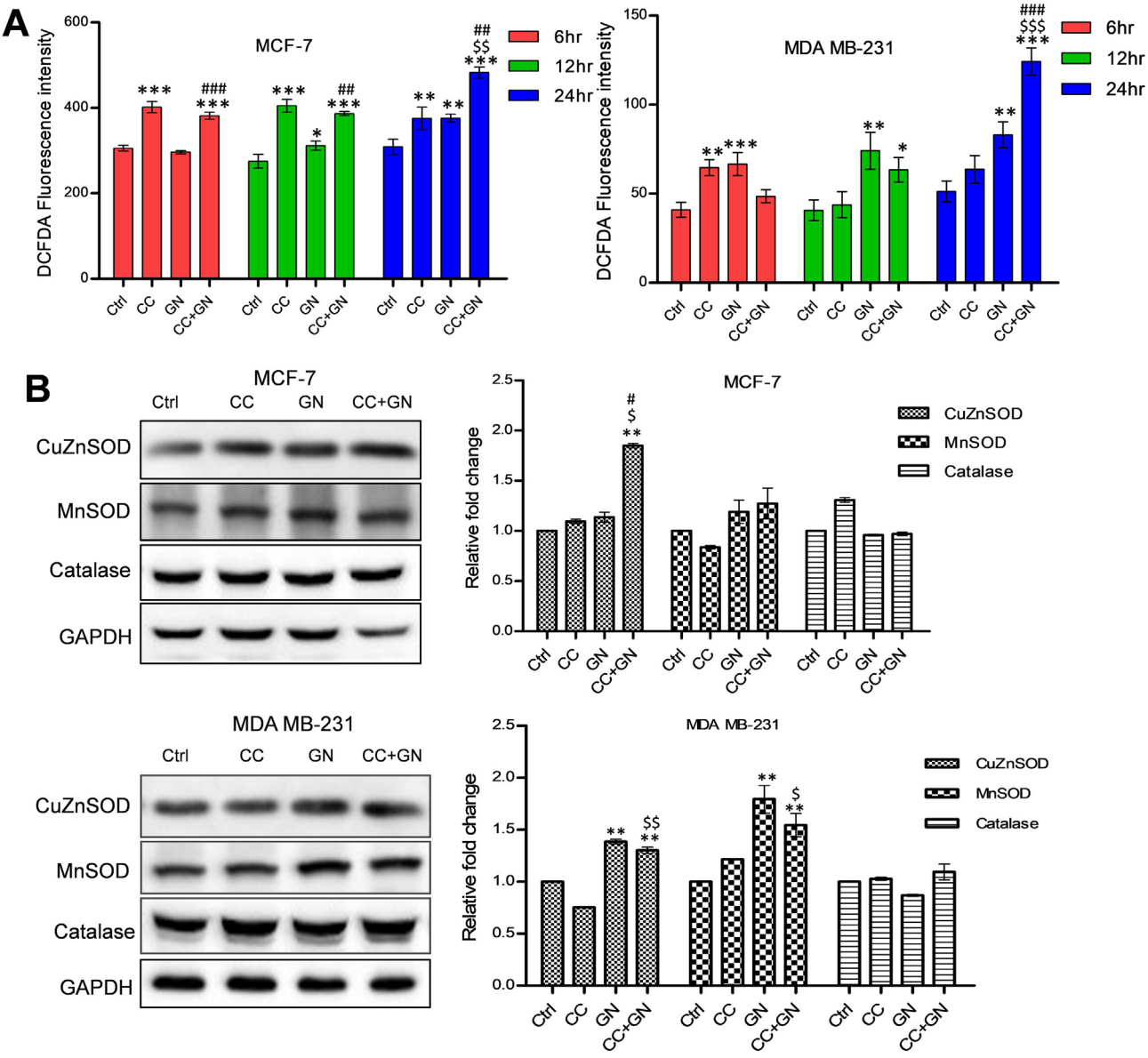

Fig. 3. Combination alters reactive oxygen species (ROS) generation. (A) After incubation with the indicated drugs for 6, 12 & 24 h, MCF-7/MDA MB-231 cells were stained with DCFDA and analyzed through flow cytometer. (B) CuZnSOD, MnSOD and catalase protein expression levels were determined using western blot analysis, GAPDH was used as loading control. Graph represents densitometric analysis of the respective proteins. Data shown are mean ± SD is one of three similar experiments. $^{*}p < 0.05$; $^{**}p < 0.01$; $^{***}p < 0.001$, calculated compared to control. $\$p < 0.05$; $\$\$p < 0.01$; $\$\$\$p < 0.001$ with respect to CC alone and $\#p < 0.05$; $\#\#p < 0.01$; $\#\#\#p < 0.001$ with respect to GN alone.

instructions. Following treatment, cells were washed with PBS and incubated with MitoTracker Deep Red FM (200 nM) for 30 min. Analysis for mean fluorescence intensity was done using FACS caliber instrument [16].

2.9. Cytochrome c release & caspase activity assay

To evaluate the release of cytochrome *c* from mitochondria, untreated and treated cells were collected by trypsinization and centrifuged at 600*g* for 5 min at 4 °C. Thereafter, cytosolic and mitochondrial fractions were isolated per manufacturer's instructions (BioVision Incorporated, 155 S. Milpitas Boulevard, Milpitas, CA 95035 USA) and protein was quantified. Subsequently, 10 µg of protein was western blotted against anti-Cytochrome-c antibody.

Activation of caspase-3, -8 &-9 were assayed using Caspase-3/CPP32, FLICE/Caspase-8 and Caspase-9 Colorimetric Assay Kit respectively (BioVision Research Products, 980 Linda Vista Avenue, Mountain View, CA 94043 USA). Following incubation with the drugs, cells were processed per manufacturer's instructions and absorbance was measured at 405 nm on SpectraMAX M2^{e} Microplate Reader.

2.10. Western blot analysis

50 µg protein per lane was processed for western blotting by SDS-PAGE and electro-transferred to PVDF membranes. After blocking with 5% bovine serum albumin, membranes were incubated with indicated primary antibodies and peroxidase-linked appropriate secondary antibody respectively. The protein expression was visualized using Immobilon Western Chemiluminescence horseradish peroxidase kit and scanned by chemidoc. Densitometric analysis for determination of relative protein expression was done using Image J software [17].

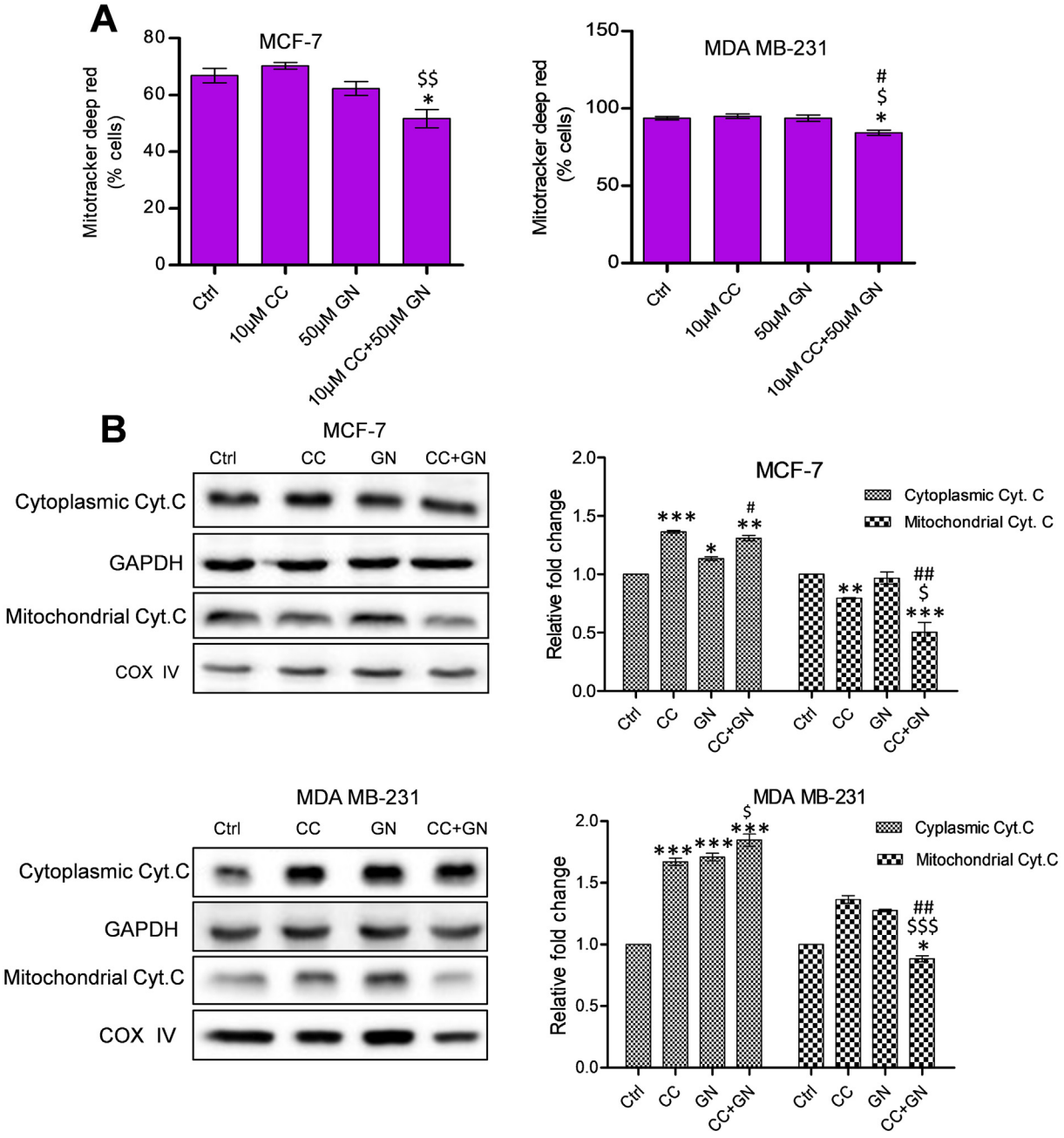

Fig. 4. (A). Analysis of mitochondrial membrane potential (MMP) has been done through mitotracker deep red FM. (B) Expression of cytochrome *c* in mitochondrial & cytosolic fraction. Data shown are mean ± SD is one of three similar experiments. *$p < 0.05$; **$p < 0.01$; ***$p < 0.001$, calculated compared to control. $$p < 0.05$; $$$p < 0.01$; $$$$p < 0.001$ with respect to CC alone and #$p < 0.05$; ##$p < 0.01$; ###$p < 0.001$ with respect to GN alone.

2.11. Transmission electron microscopic analysis

Treated MDA MB-231 cells were fixed in a mixture of 2% glutaraldehyde and 2% paraformaldehyde for 2 h at 4 °C and again post fixed in 1% osmium tetroxide at 4 °C for 1 h. Following acetone dehydration, samples were infiltrated and embedded in araldite CY 212 (TAAB, UK). Ultrathin sections were cut, mounted onto 300 mesh-copper grids and sections were stained with ethanolic uranyl acetate & alkaline lead citrate. Subsequently, samples were examined under a Morgagni 268D transmission electron microscope (Fei Company, The Netherlands).

2.12. Tumor regression study

This study was conducted according to the guidelines and standard procedures approved by the Institutional Animal Ethics Committee (IAEC), CSIR-Central Drug Research Institute, Lucknow, India. Briefly, 4T1 (7×10^5) cells were injected onto the left mammary fat pad of adult female BALB/c mice [14]. After a week, animals were randomly divided into four groups ($N = 6$) and oral dosing initiated. The two experimental groups were administered CC (10 mg/kg) and GN (200 mg/kg) alone however, the third group administered CC (10 mg/kg) plus GN (200 mg/kg) while control received saline only. Dosing was done thrice a week for 3 weeks and tumor volume was measured twice-a-week using a formula, $V = \pi/6$ (Length) × (Width)^2. Animals were observed for behavioral changes, their body weights during the study period and their survival rates were noted. The effect of treatments on the food and water intake was also observed during the experimental period. At the end of experiment, mice were sacrificed, tumors were

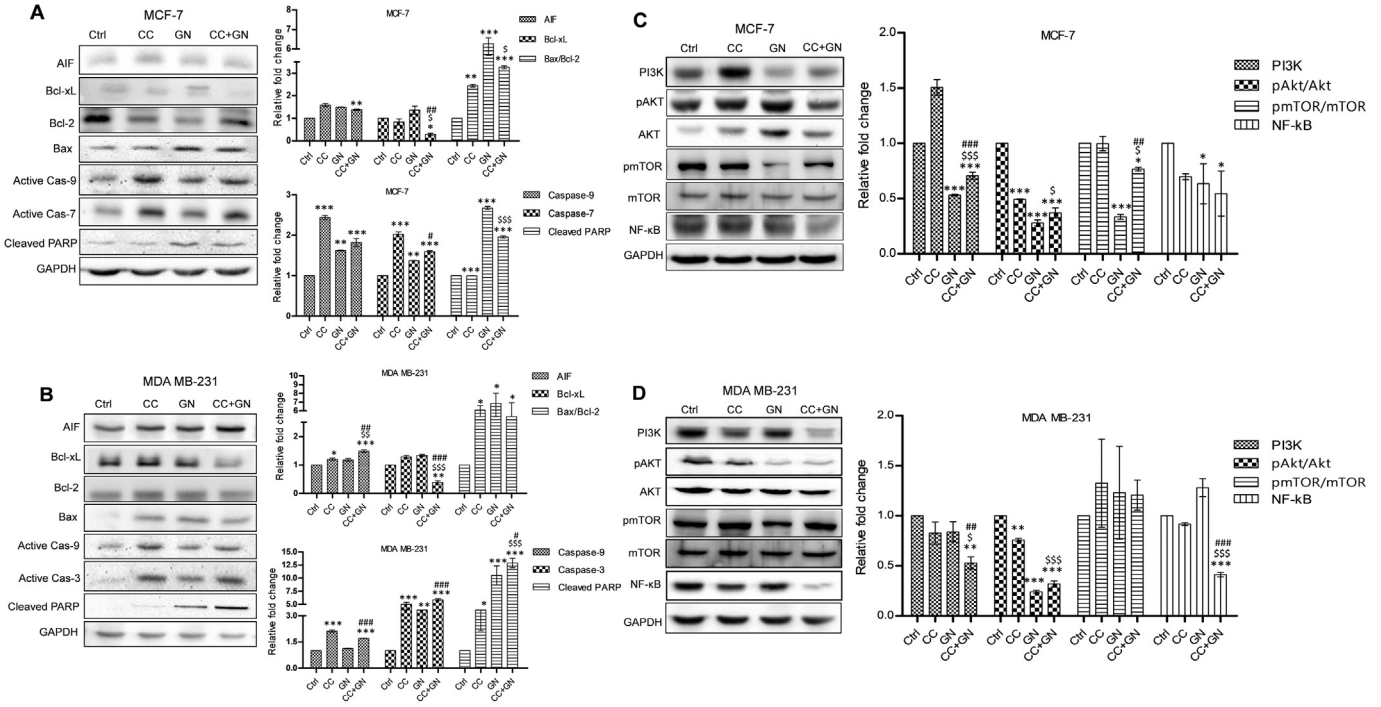

Fig. 5. Combination modulates the expression of proteins involved in apoptosis and cell survival. (A) Western blot analysis of MCF-7/MDA MB-231 cells exposed to 10 μM CC & 5 μM GN separately and together. (A & B) Expression of pro and anti-apoptotic proteins (C & D) expression of cell survival proteins. GAPDH was used as loading control. Graphical representations are indicative of relative band intensity compared to control. Data shown are mean ± SD is one of three similar experiments. $*p < 0.05$; $**p < 0.01$; $***p < 0.001$, calculated compared to control. $\$p < 0.05$; $\$\$p < 0.01$; $\$\$\$p < 0.001$ with respect to CC alone and $\#p < 0.05$; $\#\#p < 0.01$; $\#\#\#p < 0.001$ with respect to GN alone.

excised, weighed and photographed.

2.13. Statistical analysis

The results are expressed as Mean ± SD from one of three similar experiments each performed in triplicate. Oneway Analysis of Variance (ANOVA) was applied to analyze Bonferroni's Multiple Comparison Test. A statistically significant difference was defined as $p < 0.05$.

3. Results

3.1. Combination synergistically induces cytotoxicity and arrests cells in G2/M phase

The results presented here and our earlier data suggest that CC plus GN cause synergistically enhanced cytotoxicity than control and CC/GN alone in human MCF-7/MDA MB-231 HBCCs & 4T1 mouse breast cancer cells (Fig. 1A) [13]. More, safety of this combination in MCF-10A non-tumorigenic breast cells was also observed. Since the combination inhibited breast cancer cells proliferation, we next performed cell cycle analysis to check the effect of CC plus GN in different phases of cell cycle. Our results revealed remarkable increase in HBCCs at G2/M phase (Fig. 1B). Further, western blot analysis demonstrated the downregulation of cyclin B1 and up-regulation of phospho-cdc2 expression (Fig.1C). In addition, a sub-G0/G1 DNA peak suggestive of apoptotic DNA was also noticed (Fig.1D).

3.2. GN augments CC mediated apoptosis in HBCCs

Following treatment with 10 μM CC plus 50 μM GN, HBCCs displayed characteristic signs of apoptosis such as shrinkage, cell membrane blebbing and rounding (Fig. 2A) including externalization of phosphatidyserine as observed through Annexin V/PI staining (Fig. 2B).The nuclear and mitochondrial morphological changes were further subjected to transmission electron microscopy (TEM) & analyzed. As shown in Fig. 2C, control group showed prominent nucleoli with intact nuclear membrane and healthy mitochondria. Normal nuclear morphology and mitochondrial swelling was observed in CC and GN alone treated groups. In contrast, the combination group displayed chromatin condensation with loss of nucleoli and disruption in mitochondrial structural integrity with mitochondrial inflammation and damaged cristae (Fig. 2C). DNA fragmentation is the unique feature of late stage apoptosis therefore, to further reveal the combination mediated apoptosis, terminal deoxynucleotidyl transferase dUTP nick end labeling (TUNEL) assay was performed. Higher number of tunel positive cells *viz.* 17% MCF-7, 24% MDA MB-231tunel positive cells were obtained *versus* 1.97 & 0.64% respective controls (Fig. 2D).

3.3. GN enhances CC induced apoptosis through generation of reactive oxygen species (ROS) and disruption of mitochondrial membrane potential ($\Delta\psi_m$)

Significant ROS generation was encountered at 6 & 12 h in MCF-7 & MDA MB-231 cells respectively which peaked at 24 h (Fig. 3A). In addition, upregulation in CuZnSOD expression and no changes in catalase expression was observed through immunoblotting in both cell types. However, upregulation in MnSOD was found in MDA MB-231 cells only (Fig. 3B).

Elevated ROS generation causes oxidative stress and disrupts MMP which was determined using MitoTracker Deep Red FM. Combination resulted into rapid dissipation of $\Delta\psi_m$ in both MCF-7 as well as MDA MB-231 cells (Fig. 4A). Furthermore, as in Fig. 4B, the extent of cytosolic cytochrome *c* increased with concomitant decline in mitochondrial fraction in combination compared to control and mono treatment in both cells.

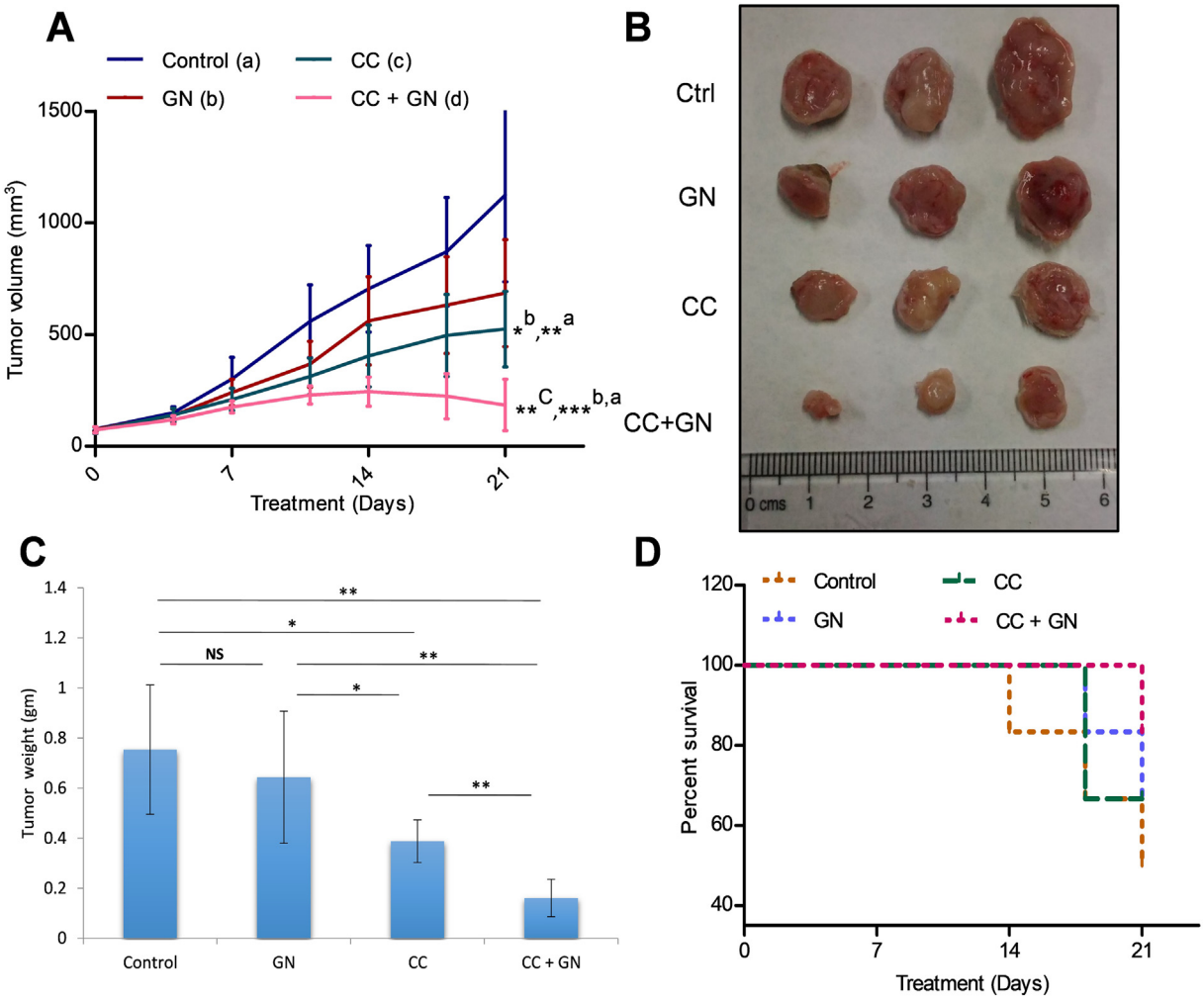

Fig. 6. Combination of CC plus GN inhibits *in vivo* tumor growth in 4 T1-syngeneic mice. 4T1 cells were inoculated in the mammary fat pad of BALB/c mice. 10 mg/kg of CC and/or 200 mg/kg GN by oral route were administered thrice-a-week for 3 weeks. Tumor volume and animal survival was noted throughout the study period. (A) Tumor volume at different time points of study. (B) The representative tumors from each group were aligned and photographed. (C) Tumor weight in different groups at the end of study. (D) Kaplan-Meier survival chart showing percentage survival probability for all test groups of animals. $*p < 0.05$; $**p < 0.01$; $***p < 0.001$, calculated compared to control (a), GN (b), CC (c) and GN + CC (d).

3.4. Combination alters expression of Bcl-2 family proteins, activates caspases and induces PARP cleavage

In order to further delineate the molecular pathways involved in combination mediated apoptosis, western blot analysis was performed. As shown in Fig. 5A & B, combination of CC plus GN significantly up-regulated Bax expression however, anti-apoptogenic Bcl-2 and Bcl-xL expression was down-regulated in HBCCs. Moreover, densitometry analysis shows upsurge in Bax/Bcl-2 ratio in combination compared to control. Caspase activity assay was undertaken to ascertain the role of caspases in combination mediated apoptosis. The result demonstrates that combination activated caspase-9 in both MCF-7/MDA MB-231 cells and caspase-3 in the latter only (Supplementary Fig. 1). Conversely, no significant alteration in caspase-8 activity was observed in either cell lines as examined using SRB assay (Supplementary Fig.1). To further substantiate the results, immunoblotting was performed for active caspases 3/7 & -9. The results illustrate that combination significantly up-regulated the expression of caspase-7 & 9 in MCF-7 cells (Fig. 5A) and caspase-3 &-9 in MDA MB-231 cells (Fig.5B). We also analyzed the expression of AIF, another downstream regulator of apoptosis [18]. Significant expression of AIF was noticed in combination *versus* control in MCF-7/MDA MB-231 cells. In addition, the cleavage of full length PARP into characteristic 89 kDa fragment, another classical marker, was also observed in combination treatment in both cells (Fig. 5A & B).

3.5. Combination efficiently abrogates PI3K/Akt/mTOR/NF-κB signaling

To elucidate the basis of the potentiated anti-tumorigenic effects of CC plus GN in MCF-7/MDA MB-231 cells, we analyzed its effect on the expression of proteins involved in cell survival pathway. PI3K/Akt pathway plays an important role in cancer progression by sustaining cell proliferation, averting apoptosis and supporting the process of metastasis [19]. Aberrant activation of the PI3K/Akt frequently occurs in breast cancer where current efforts have focused on development of new anticancer agents directing this pathway. Thus, the effect of combination on PI3K/Akt/mTOR pathway was investigated. The result showed that combination decreases phosphorylation of PI3K and Akt in both the cell lines (Fig. 5C & D) whereas, decreased phosphorylation of mTOR was noticed only in MCF-7 cells (Fig. 5C). In addition, we also investigated expression of NF-κB, a key regulator of cell proliferation whose action is partly mediated through AKT signaling pathway. The result displayed significant down-regulation of NF-κB in combination in both cells *versus* control (Fig. 5C & D).

3.6. Combination reduced breast cancer growth in mouse 4T1 breast tumor model

Tumor regression study was undertaken to evaluate the efficacy of CC plus GN in 4T1 syngeneic mouse model. The animals behaved normally and there was no noticeable effect of treatment on the food and water intake in mice compared to control group. The relative weight of mice *versus* time is indicated in Supplementary Fig. 3 that was aimed to assess the *in vivo* toxicity of the treatment. All the treatment groups were found not to be toxic at the doses studied, as we did not observe body weight reduction in the mice. As shown in Fig. 6A, B & C combination significantly inhibited the growth of tumor compared to control and CC/GN alone by diminishing the volume and weight of the tumors. About 6.09, 4.15and 2.88 fold higher regression was obtained in combination compared to control, GN and CC alone groups respectively. Additionally, at the end of the study, combination reduced the tumor weight by 4.67, 4 and 2.40 fold compared to control, CC and GN alone groups respectively (Fig. 6C). Combination successfully enhanced the survival of animals in our study (Fig. 6D), as the percentage of animals died till the end of the study was lowest in this group.

4. Discussion

Emerging evidences including our work suggests employment of natural compounds such as genistein, resveratrol, curcumin, daidzein *etc.* during radio- or chemotherapy for enhanced efficacy and reduced toxicity [12]. Several studies have demonstrated that dietary isoflavone genistein (GN) possesses anticancer properties against many cancers including breast, collateral safety to normal cells enabling its use in conjunction with other therapies. Centchroman (CC) or Ormeloxifene exhibits anticancer action against wide range of cancers. Herein, we assessed the efficacy of CC in combination with GN against ER + ve/-ve MCF-7/MDA MB-231 HBCCs *in vitro* and in a mouse 4T1 breast tumor model *in vivo*. Although CC and GN alone effectively inhibit cell growth, supplementation of GN remarkably enhanced CC induced cell killing as confirmed by *in vivo* studies too.

Inhibition of cell cycle regulation represents a desirable target for management of breast cancer [20]. Our results show that combination arrests HBCCs at G2/M phase, depletes cyclin B1 and increases phospho cdc2 (Fig. 1B & C). Liu X et al. have also reported that GN improves the radiosensitivity of HBCCs through similar mechanisms [9]. Inhibition of apoptosis is a major hallmark of cancer [21]. We and others have reported that CC inhibits breast, endometrial, pancreatic and head & neck cancer cells growth by inducing apoptosis [6,7]. Herein, our result reveal that combination of CC plus GN induced higher apoptosis compared to each drug *per se*, evidenced by Annexin V/PI staining (Fig. 2B). Further, alteration in nuclear morphology and high DNA fragmentation in CC plus GN treated groups substantiates the foregoing (Fig. 2C & D). These results are consistent with our previous findings that daidzein/resveratrol/curcumin augments apoptotic potential of CC in MCF-7/MDA MB-231 HBCCs [22,23].

Presently, we provide additional novel mechanistic insights into synergism between CC and GN in HBCCs. Our results indicate higher ROS generation in combination after 24 h of treatment in both the cell types (Fig. 3A & B). This observation is in line with the fact that ROS generation precedes apoptosis [24]. To further explore this, we examined the role of combination on mitochondrial membrane potential (MMP) which decreased with concomitant release of cytochrome *c* from mitochondria, indicating activation of apoptosis (Fig. 4A & B). It has been established that the balance between pro- and anti-apoptotic members of the Bcl-2 family proteins regulate the mitochondrial membrane permeabilization [25,26]. As expected, combination decreased the expression of anti-apoptotic proteins Bcl-2 and Bcl-xL with increased pro-apoptotic Bax expression (Fig. 5A & B).We previously reported similar findings of CC mediated down regulation of Bcl-2 and up-regulation of Bax expression [7]. Caspases, the members of a cysteine protease family are known to be the major regulators of apoptosis [27,28]. Several studies including ours have demonstrated that anticancer agents up regulate caspases especially, -3, -8 &-9 [6,7]. In this study, the results suggest that CC plus GN significantly activate Caspase-3 & -9 in HBCCs (Supplementary Fig. 1), indicating their pivotal role in apoptosis, reaffirmed by western blotting (Fig. 5A & B).

Studies have shown that GN and other dietary compounds which inhibit cancer growth may augment the efficacy of cancer chemotherapeutics by altering the action of leading cell survival pathways such as PI3K/Akt/mTOR and those controlled by NF-κB [29]. Furthermore, studies from various laboratories suggest that inhibition of Akt/NF-κB leads to up-regulation of Bax and down-regulation of Bcl-2 [30,31]. CC also has been found to induce cell death by inhibition of PI3K/mTOR pathway in Head & Neck cancer cells [8]. Here, combination inhibited PI3K, Akt and mTOR (Fig. 5C & D) which further down and up-regulated the expression of Bcl-2 and Bax respectively thereby synergistically inducing apoptosis in HBCCs. Combination mediated inhibition of Akt leads to activation of caspase-9, promoting apoptosis supported by similar observations [32]. Several reports have shown that activation of NF-κB encourages cell survival and proliferation whose down-regulation sensitizes the cells for apoptosis [33,34]. It has been reported that GN increases apoptosis induced by chemotherapeutic agents by inactivation of NF-κB in human cancer cells [11]. Our results also revealed that GN synergizes CC action by down-regulating the expression of NF-κB (Fig. 5C & D). These studies have also been supported using appropriate inhibitors for diverse pathways (Supplementary Fig. 2). Finally, we demonstrated the CC plus GN induced synergistic inhibition of tumor growth in mouse 4T1 breast tumor model with adequate tolerance (Fig. 6A–D).

In conclusion, we revealed the mechanism of action of a novel combination of CC and GN in HBCCs by which combination inhibits cell growth by arresting cells in G2/M phase, inhibiting PI3k/Akt expression as well as inducing apoptosis by ROS dependent mitochondrial pathway. Our *in vitro* results are well supported by *in vivo* findings where it was found that combination efficiently inhibits tumor growth. The combination treatment of CC and GN caused significant tumor regression compared to control & CC/GN alone and was well tolerated. Also, there was reduction in the mortality of mice in combination group during the study period compared to other groups. Therefore, the combination of CC with GN offers a novel approach for Breast Cancer since the *in vitro* derived results translate into *in vivo* facts and may potentially establish new possibilities for further translational research.

Acknowledgements

We would like to thank Mr. A. L. Vishwakarma for his help in experiments with flow cytometry. Shweta Kaushik gratefully acknowledges the fellowship received from UGC, New Delhi.

Funding

This research was supported by the funds from MLP-0750, CSIR-Central Drug Research Institute, Lucknow, India.

Authors contribution

Conception and design: Shweta Kaushik, Ramesh Sharma, Hari Shyam and Anil K. Balapure.

Development of methodology: Shweta Kaushik, Hari Shyam and Anil K. Balapure.

Acquisition of data: Shweta Kaushik, Satish Agrawal, Anil K. Dwivedi and Tapas C Nag.

Writing, review and/or revision of the manuscript: Shweta Kaushik, Hari Shyam and Anil K. Balapure.

Study supervision: Anil K. Balapure.

Declaration of competing interest

The authors declare no potential conflict of interest.

Appendix A. Supplementary data

Supplementary data to this article can be found online at https://doi.org/10.1016/j.lfs.2019.117073.

References

[1] F. Bray, J. Ferlay, I. Soerjomataram, R.L. Siegel, L.A. Torre, A. Jemal, Global cancer statistics 2018: GLOBOCAN estimates of incidence and mortality worldwide for 36 cancers in 185 countries, CA Cancer J. Clin. 68 (2018) 394–424.

[2] T.R. Wilson, D.B. Longley, P.G. Johnston, Chemoresistance in solid tumours, Annals of Oncology: Official Journal of the European Society for Medical Oncology/ESMO. 17 (Suppl. 10) (2006) x315–x324.

[3] M.M. Singh, Centchroman, a selective estrogen receptor modulator, as a contraceptive and for the management of hormone-related clinical disorders, Med. Res. Rev. 21 (2001) 302–347.

[4] S. Agrawal, H. Ahmad, M. Dwivedi, M. Shukla, A. Arya, K. Sharma, et al., PEGylated chitosan nanoparticles potentiate repurposing of ormeloxifene in breast cancer therapy, Nanomedicine. 11 (2016) 2147–2169.

[5] S. Khan, M.C. Ebeling, N. Chauhan, P.A. Thompson, R.K. Gara, A. Ganju, et al., Ormeloxifene suppresses desmoplasia and enhances sensitivity of gemcitabine in pancreatic cancer, Cancer Res. 75 (2015) 2292–2304.

[6] M. Nigam, V. Ranjan, S. Srivastava, R. Sharma, A.K. Balapure, Centchroman induces G0/G1 arrest and caspase-dependent apoptosis involving mitochondrial membrane depolarization in MCF-7 and MDA MB-231 human breast cancer cells, Life Sci. 82 (2008) 577–590.

[7] H. Shyam, N. Singh, S. Kaushik, R. Sharma, A.K. Balapure, Centchroman induces redox-dependent apoptosis and cell-cycle arrest in human endometrial cancer cells, Apoptosis. 22 (2017) 570–584.

[8] V.K. Srivastava, R.K. Gara, M.L. Bhatt, D.P. Sahu, D.P. Mishra, Centchroman inhibits proliferation of head and neck cancer cells through the modulation of PI3K/mTOR pathway, Biochem. Biophys. Res. Commun. 404 (2011) 40–45.

[9] X. Liu, C. Sun, X. Jin, P. Li, F. Ye, T. Zhao, et al., Genistein enhances the radiosensitivity of breast cancer cells via G(2)/M cell cycle arrest and apoptosis, Molecules. 18 (2013) 13200–13217.

[10] S. Banerjee, Y. Zhang, S. Ali, M. Bhuiyan, Z. Wang, P.J. Chiao, et al., Molecular evidence for increased antitumor activity of gemcitabine by genistein in vitro and in vivo using an orthotopic model of pancreatic cancer, Cancer Res. 65 (2005) 9064–9072.

[11] Y. Li, F. Ahmed, S. Ali, P.A. Philip, O. Kucuk, F.H. Sarkar, Inactivation of nuclear factor kappaB by soy isoflavone genistein contributes to increased apoptosis induced by chemotherapeutic agents in human cancer cells, Cancer Res. 65 (2005) 6934–6942.

[12] F.H. Sarkar, Y. Li, Using chemopreventive agents to enhance the efficacy of cancer therapy, Cancer Res. 66 (2006) 3347–3350.

[13] S. Kaushik, H. Shyam, R. Sharma, A.K. Balapure, Genistein synergizes centchroman action in human breast cancer cells, Indian Journal of Pharmacology. 48 (2016) 637–642.

[14] S. Khan, S. Shukla, S. Sinha, A.D. Lakra, H.K. Bora, S.M. Meeran, Centchroman suppresses breast cancer metastasis by reversing epithelial-mesenchymal transition via downregulation of HER2/ERK1/2/MMP-9 signaling, Int. J. Biochem. Cell Biol. 58 (2015) 1–16.

[15] N. Singh, M. Nigam, V. Ranjan, D. Zaidi, V.K. Garg, S. Sharma, et al., Resveratrol as an adjunct therapy in cyclophosphamide-treated MCF-7 cells and breast tumor explants, Cancer Sci. 102 (2011) 1059–1067.

[16] N. Singh, J. Kaur, P. Kumar, S. Gupta, N. Singh, A. Ghosal, et al., An orally effective dihydropyrimidone (DHPM) analogue induces apoptosis-like cell death in clinical isolates of Leishmania donovani overexpressing pteridine reductase 1, Parasitol. Res. 105 (2009) 1317–1325.

[17] J. Dewangan, S. Kaushik, S.K. Rath, A.K. Balapure, Centchroman regulates breast cancer angiogenesis via inhibition of HIF-1alpha/VEGFR2 signalling axis, Life Sci. 193 (2018) 9–19.

[18] J.F. Kerr, A.H. Wyllie, A.R. Currie, Apoptosis: a basic biological phenomenon with wide-ranging implications in tissue kinetics, Br. J. Cancer 26 (1972) 239–257.

[19] X. Li, C. Wu, N. Chen, H. Gu, A. Yen, L. Cao, et al., PI3K/Akt/mTOR signaling pathway and targeted therapy for glioblastoma, Oncotarget. 7 (2016) 33440–33450.

[20] G.K. Schwartz, M.A. Shah, Targeting the cell cycle: a new approach to cancer therapy, Journal of Clinical Oncology: Official Journal of the American Society of Clinical Oncology. 23 (2005) 9408–9421.

[21] D. Hanahan, R.A. Weinberg, Hallmarks of cancer: the next generation, Cell. 144 (2011) 646–674.

[22] S. Kaushik, H. Shyam, R. Sharma, A.K. Balapure, Dietary isoflavone daidzein synergizes centchroman action via induction of apoptosis and inhibition of PI3K/Akt pathway in MCF-7/MDA MB-231 human breast cancer cells, Phytomedicine. 40 (2018) 116–124.

[23] N. Singh, D. Zaidi, H. Shyam, R. Sharma, A.K. Balapure, Polyphenols sensitization potentiates susceptibility of MCF-7 and MDA MB-231 cells to Centchroman, PLoS One 7 (2012) e37736.

[24] H. Zhang, C. Gajate, L.P. Yu, Y.X. Fang, F. Mollinedo, Mitochondrial-derived ROS in edelfosine-induced apoptosis in yeasts and tumor cells, Acta Pharmacol. Sin. 28 (2007) 888–894.

[25] A.W. Leung, A.P. Halestrap, Recent progress in elucidating the molecular mechanism of the mitochondrial permeability transition pore, Biochim. Biophys. Acta 1777 (2008) 946–952.

[26] F. Ricchelli, J. Sileikyte, P. Bernardi, Shedding light on the mitochondrial permeability transition, Biochim. Biophys. Acta 1807 (2011) 482–490.

[27] G.M. Cohen, Caspases: the executioners of apoptosis, The Biochemical Journal. 326 (Pt 1) (1997) 1–16.

[28] S. Elmore, Apoptosis: a review of programmed cell death, Toxicol. Pathol. 35 (2007) 495–516.

[29] A. Ahmad, B. Biersack, Y. Li, D. Kong, B. Bao, R. Schobert, et al., Targeted regulation of PI3K/Akt/mTOR/NF-kappaB signaling by indole compounds and their derivatives: mechanistic details and biological implications for cancer therapy, Anti Cancer Agents Med. Chem. 13 (2013) 1002–1013.

[30] B.F. El-Rayes, S. Ali, I.F. Ali, P.A. Philip, J. Abbruzzese, F.H. Sarkar, Potentiation of the effect of erlotinib by genistein in pancreatic cancer: the role of Akt and nuclear factor-kappaB, Cancer Res. 66 (2006) 10553–10559.

[31] B.N. Fahy, M.G. Schlieman, M.M. Mortenson, S. Virudachalam, R.J. Bold, Targeting BCL-2 overexpression in various human malignancies through NF-kappaB inhibition by the proteasome inhibitor bortezomib, Cancer Chemother. Pharmacol. 56 (2005) 46–54.

[32] D. Subramaniam, G. Kaushik, P. Dandawate, S. Anant, Targeting cancer stem cells for chemoprevention of pancreatic cancer, Curr. Med. Chem. 24 (2017).

[33] B.B. Aggarwal, Nuclear factor-kappaB: the enemy within, Cancer Cell 6 (2004) 203–208.

[34] B.B. Aggarwal, S. Shishodia, Molecular targets of dietary agents for prevention and therapy of cancer, Biochem. Pharmacol. 71 (2006) 1397–1421.